Available online at www.sciencedirect.com
SCIENCE DIRECT®
Bioorganic & Medicinal Chemistry 13 (2005) 2679–2689
Bioorganic & Medicinal Chemistry

The study on the interaction between seryl-histidine dipeptide and proteins by circular dichroism and molecular modeling

Qing Zeng, Qiang Yin and Yufen Zhao*

The Key Laboratory of Bioorganic Phosphorus Chemistry, Ministry of Education, China, Department of Chemistry, School of Life Sciences and Engineering, Tsinghua University, Beijing 100084, China

Received 30 November 2004; revised 21 December 2004; accepted 23 December 2004

Abstract—The selective cleavage of proteins is very important in key biological processes. Chemical (nonenzymatic) reagents such as cyanogen bromide and transition metal complexes are used extensively with great defects. In this paper, the binding of seryl-histidine dipeptide (abbreviated as SH) with bovine serum albumin (BSA) and lysozyme were investigated by the circular dichroism spectroscopy (CD) at 298 K, molecular docking studies and quantum chemical calculations based on the previous results of polyacrylamide gel electrophoresis (PAGE). From the studies of CD, it showed that SH interacted strongly with BSA and lysozyme. The change percentages of the secondary structures of BSA and lysozyme were calculated. The contents of the β-sheets decreased remarkably. It indicated that the interactions between SH and proteins could break the hydrogen bonds of β-sheets selectively. The docking studies between SH and BSA showed that the position of the oxygen atom of the hydroxyl group of SH (O_{12}) was in favor of a nucleophilic attack on carbon atom of the amide bond of a β-sheet (C_{34}) because the distance between O_{12} and C_{34} was 3.37 Å. Natural charges, natural atomic hybrid percentages and square sums of HOMO coefficients calculated by the NBO and population analysis at HF/6-31G* supported the suggested mechanism. And so SH may be an interesting agent for the therapeutic use.

1. Introduction

Hydrolysis of the inactivated amide bond in peptides and proteins is an extremely slow reaction. The half-life of it in neutral solution is about hundreds of years.[1] However, the hydrolytic reaction is an essential metabolic process and a desirable reaction in various bioanalytical procedures. The reagents are usually proteases that affect it both in vivo and in vitro.[2,3] As one of the largest and most important groups of enzymes, proteases play significant roles in mediating different cellular processes such as DNA replication, cell-cycle progression, cell proliferation, differentiation, and migration etc.,[4] therefore, many fatal diseases such as emphysema, stroke, viral infections, cancer and Alzheimer's disease are associated with the malfunctioning of the cellular proteolytic system. Almost one-third of all proteases can be classified as serine proteases, named for the nucleophilic Ser residue at the active site. This mechanistic class was originally distinguished by the presence of the Asp-His-Ser catalytic triad.[5] More recently, serine proteases with novel catalytic triads and dyads have been discovered, including Ser-His-Glu, Ser-Lys/His, His-Ser-His, and N-terminal Ser.[6] The roles of Ser (or related amino acid residues) and His are well documented in the peptide bond and ester bond cleavage reactions of serine proteases, lipases, esterases, and other polypeptide enzymes.[7]

However, only a few proteases such as trypsin[8] are routinely applicable in biochemistry and structural biology. They have great catalytic power, but their sequence selectivity can be changed with difficulty, and their size and activities under particular pH values and temperatures may limit their use as probes of molecular structures and interactions. Furthermore, since the requirements for traditional applications are changing today, new methods for selective cleavage of peptides and proteins are needed to be found for many tasks in analytic biochemistry and molecular biology,[9] for example, semisynthesis of proteins, the sequencing of large or blocked protein, structural and functional analysis of protein domains, the development of new drugs, etc. Moreover, the mechanism of many fatal diseases such

Keywords: Seryl-histidine dipeptide; Protein secondary structure; Circular dichroism spectroscopy; Molecular docking study.
* Corresponding author. Tel.: +86 10 62772259; fax: +86 10 62781695; e-mail addresses: zq68315@yahoo.com.cn; zq68315@mail.tsinghua.edu.cn

0968-0896/$ - see front matter © 2005 Elsevier Ltd. All rights reserved.
doi:10.1016/j.bmc.2004.12.047

as prion and Alzheimer's is related to the aggregation of α-helix-rich proteins into β-sheet-rich amyloid fibrils.[10–12] Since some small molecules have been used to interfere with the aggregation,[11,13] chemical (nonenzymatic) reagents such as cyanogen bromide and transition metal complexes are used extensively. But cyanogen bromide is volatile and toxic, it requires harsh conditions, and often produces incomplete cleavage. Metal complexes are rarely used to directly and selectively hydrolyze proteins due to the cleavage difficulty. Up to now, it has been reported that only four proteins can be really hydrolyzed by transition metal complexes.[14]

In our laboratory, an important finding has been reported that the dipeptide Ser-His (SH) is the shortest peptide which has multiple cleavage activities. That is, Ser-His itself can cleave DNA, RNA, protein and a carboxyl ester.[7,15–17] SH can retain its multiple cleavage activities when amino acids are added internally or to its C-terminus. It demonstrates the extraordinary evolutionary capacity of SH. Since the number of catalytically active combinations available for the evolution of polypeptide enzymes is limited due to the relatively small number of functional groups provided by the natural amino acids, the successful combination of Ser and His is probably and repeatedly selected in the evolution of diverse groups of enzymes.

In the current work, two proteins were used to do the research. One was bovine serum albumin (BSA). The other was lysozyme. Serum albumins including bovine (BSA) and human serum albumins (HSA) are the most abundant of the proteins in blood plasma, accounting for about 60% of the total protein corresponding to a concentration of 42 g/L, and they provide about 80% of the osmotic pressure of blood.[18] They play an important role in the transport and deposition of many endogenous and exogenous substances in blood due to the existence of a limited number of binding regions but very different specificity.[19,20] They have the interesting properties of binding a variety of hydrophobic ligands such as fatty acids, lysolecithin, bilirubin, warfarin, tryptophan, steroids, anaesthetics, and several dyes.[18] Since the overall distribution, metabolism, and efficacy of many drugs in the body are correlated with their affinities towards serum albumins, the investigation of pharmaceuticals with respect to albumin–drug bonding is imperative and fundamentally important.[21]

Lysozyme is an important bacteriolytic agent found in various body fluids and tissues. Its concentration ranges from 4 to 13 mg/L in serum and from 450 to 1230 mg/L in tears.[22] Leucocytes such as monocytes, macrophages, and polymorphonuclear granulocytes are known to synthesize and secrete lysozyme in animals. Kidney tissue appears to have the greatest concentration of lysozyme activity, likely due to the high concentration of these leucocytes in the anterior hematopoietic portion of the kidney. Due to the antibacterial properties of lysozyme and because it is located in areas that are in frequent contact with pathogens (i.e., kidney and skin mucus), it is an important factor in protecting animals against bacterial pathogens.[23] BSA and lysozyme have been used as model proteins for many and diverse biophysical, biochemical, and physicochemical studies.[9,18] Therefore, they were also selected as our model proteins on account of their lone-standing interests in the protein community.

In this article, we report the interactions between SH and proteins studied by the circular dichroism spectroscopy, molecular docking studies and quantum chemical calculations based on the previous results of PAGE. It is found that the interactions between SH and proteins can cause the breakage of the hydrogen bonds of β-sheets selectively. And it is possible that SH can cleave a protein specifically at β-sheet.

2. Results and discussion

2.1. The results of CD assays

In our previous experiments, Li et al.[7] and Chen et al.[15] had proved that BSA (5 μg) and lysozyme could be indeed cleaved by SH (10 mM) into smears of progressively smaller fragments of heterogeneous sizes, as revealed by silver-stained 10% reducing PAGE. And the optimal reaction conditions were similar to those for DNA cleavage. That is, the pH value in 40 mM Britton–Robinson (B–R) buffer was 6 for the cleavage at 37 °C. The rate of cleavage was also temperature-dependent; incubation at 50 °C for 48 h resulted in faster BSA and lysozyme cleavage than at 37 °C, and even higher rates of cleavage were observed at 60 °C. It suggests that SH can keep its cleavage activity when it is used in vivo at 37 °C (310 K). Chymotrypsin (100 nM) also had strong cleavage activity when it was incubated with BSA (5 μg) and B–R buffer (pH 7.8) at 37 °C for 40 min. Other related oligopeptides were tested for proteolytic activity, and the results showed a consistent pattern in modifications to SH and corresponding changes in cleavage activity. In the negative control experiment without oligopeptides, BSA remained intact and could not be cleaved.

From the results of PAGE,[7] it was also found that the nucleolytic activity in samples incubated with SH had no sequence specificity. Therefore, there were many fragment ions hard to be analyzed in the experiment of mass spectrometry (MS). It was unfavorable to use MS to identify the site of cleavage in the system.

However, it was necessary to further understand some information about the conformational changes in proteins. Because the PAGE data could not reflect the results, CD experiments were performed. The same experiments were repeated five times. Two groups of parallel experimental results are listed in Table 1. It can be found that the errors represented by RMS between the experimental and conversion CD spectra are both very small (~15%). In the control experiment, BSA contains 45.7% α-helices and 26.5% β-sheets similar to the general results that the secondary structures of BSA contain 67% α-helices, six turns and 17 disulfide bridges.[18] That is, the conformation of BSA in water

Table 1. The percentages (*C*) of BSA[a] secondary structures before and after the addition of SH at 298 K

Entry	BSA	I		II	
		SH + BSA	ΔC_{BSA}[c]	SH + BSA	ΔC_{BSA}[c]
Helix	45.7	56.8	11.1	63.2	17.5
Beta	26.5	16.3	−10.2	10.9	−15.6
Turn	0.0	0.0	0.0	0.0	0.0
Random	27.8	26.9	−0.9	25.9	−1.9
Total	100.0	100.0	0.0	100.0	0.0
RMS[b]	16.8	16.3	−0.5	15.2	−1.6

[a] The mean residue concentration of BSA is 0.00018 mol/L.
[b] RMS means the error between the experimental and conversion CD spectra.
[c] ΔC=C (SH + BSA)–C (BSA).

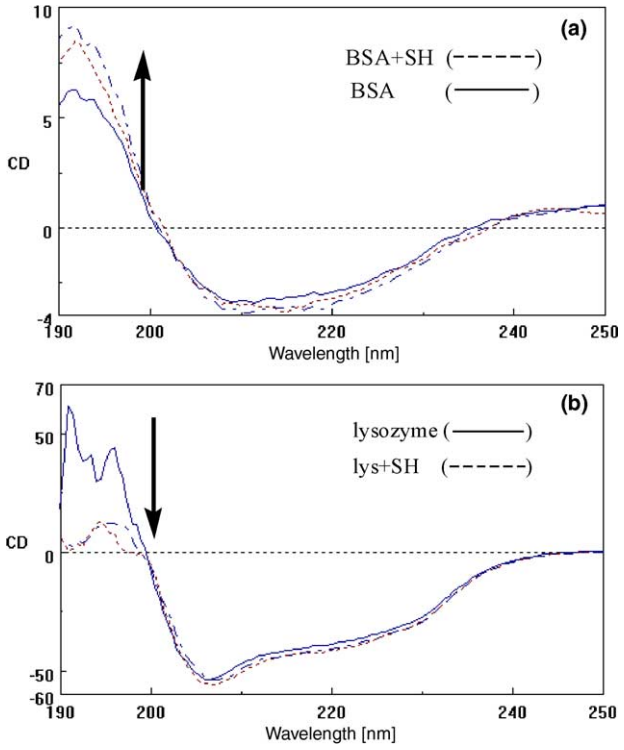

Figure 1. The CD spectra of BSA (a) and lysozyme (b) before (solid line) and after the addition of SH (dashed lines).

solution is made up of α-helices (Fig. 1a). In 191 nm, there is a positive peak. In 210 and 218 nm, there are two negative grooves. It is different from that in its crystal structure. In the main chain of BSA crystal (Protein Data Bank code: 1C1U), the contents of α-helices and β-sheets are 10.42% and 29.73%, respectively. The following molecular modeling uses its crystal structure.

The titration of SH to proteins was used. After SH was titrated into the BSA solution, the incubation time was about 5 min at 298 K until the solution reached the equilibrium state. In the first group, the percentages of α-helices of BSA increased from 45.7% to 56.8% and that of β-sheets dropped from 26.5% to 16.3%, while the contents of turn and random coils did not change much. Namely, the contents of α-helices increased 11.1% indicated by the upper arrow (Fig. 1a), and the contents of β-sheets were decreased 10.2%. In the second group, the similar results were obtained. The contents of α-helices increased 17.5% and the contents of β-sheets decreased 15.6%. It is known that pH value, temperature, and solvent can alter the secondary structure of proteins.[24,25] But these elements were kept the same before and after the addition of SH, it indicated that it was the interaction between SH and BSA that resulted in the hydrogen bond breakage of β-sheets and the conformational changes.

The similar phenomena were also observed in another experiment that SH interacted with lysozyme (Fig. 1b and Table 2). In the control experiment, lysozyme contains 14.1% α-helices and 53.2% β-sheets. In 197 and 206 nm, there are a positive peak and a negative groove, respectively. Its conformation in solution is made up of β-sheets, which is different from that in its crystal structure. In lysozyme crystal (Protein Data Bank code: 132L), the contents of α-helices and β-sheets are 31.01% and 6.20%, respectively. When SH was added to the lysozyme solution, the solution was incubated for about 5 min at 298 K. In the first group, the contents of α-helices of lysozyme increased from 14.1% to 19.0% and the percentages of β-sheets dropped from 53.2% to 26.5% greatly, and the contents of turn and random coils also increased obviously. Namely, the contents of α-helices increases 4.9% and the contents of β-sheets are decreased 26.7% indicated by the down arrow (Fig. 1b). In the second group, the similar results were obtained. The contents of α-helices only increased 4.8% and the contents of β-sheets decreased 24.9% obviously. It further indicated that the interaction between SH and β-sheets damaged the hydrogen bonds of β-sheets and resulted in the conversion of β-sheets to other secondary structures.

It has been known that prion diseases differ from other infectious diseases in that the pathogen is a proteinaceous particle, and the essential component of prions is the scrapie prion protein (PrP^{Sc}). PrP^{Sc} is chemically indistinguishable from the normal cellular prion protein (PrP^{c}). But their secondary and tertiary structures are different. Fourier transform infrared and circular dichroism spectroscopy studies indicate that PrP^{c} is highly helical (49.1%) with virtually no β-sheet structure

Table 2. The percentages (*C*) of lysozyme[a] secondary structures before and after the addition of SH at 298 K

Entry	Lysozyme	I		II	
		SH + lys	ΔC_{lys}[c]	SH + lys	ΔC_{lys}
Helix	14.1	19.0	4.9	18.9	4.8
Beta	53.2	26.5	−26.7	28.3	−24.9
Turn	4.0	19.2	15.2	18.7	14.7
Random	28.7	35.3	6.6	34.1	5.4
Total	100.0	100.0	0.0	100.0	0.0
RMS[b]	22.3	16.8	−5.5	15.7	−6.6

[a] The mean residue concentration of lysozyme is 0.00645 mol/L.
[b] RMS means the error between the experimental and conversion CD spectra.
[c] ΔC=C (SH + lys)–C (lysozyme).

(3.6%), and, in contrast, PrP^{Sc} contains a large amount of β-sheet structure (43%) and less helical structure (30%). These results, together with those of structural prediction and peptide studies led to the suggestion that a conversion of α-helices to β-sheets may occur upon formation of PrP^{Sc} from PrP^{c}. So, developing diagnostic and therapeutic agents for prion diseases are urgent and should become a reality.[26]

But we do not know how SH interacts with β-sheets specifically. If SH can cleave β-sheets selectively, it will be a very significant result. SH can be used to cure the diseases caused by the conformation changes of proteins.

2.2. The results of molecular modeling

In order to understand the key structural features that SH can interact with β-sheets selectively from atomic and molecular levels, the molecular modeling is used to investigate the interaction mechanism.

In Table 3, the binding energies of the complexes of SH with secondary structures of BSA represented by SH···BSAα, SH···BSAβ, SH···BSA*t*, and SH···BSA*c* are all negative values. It means that the conformational energies of the four complexes are all global minima in potential energy surfaces. And SH···BSAβ have the lowest binding energy (−2429.9 kcal/mol). But the energetic differences among them are not very apparent because no solvent effect was considered during the docking procedures owing to the computational limitation. Therefore, the lowest negative $E_{binding}$ is not sufficient for explaining that SH can interact with β-sheets specifically.

Table 3. The binding energies of SH with secondary structures of BSA (kcal/mol)

Entry	Nucleophilic ability of SH[a]	$E_{complex}$	$E_{binding}$[b]
Helix	–	1632.5	−2354.4
Beta	+	1557.0	−2429.9
Turn	–	1594.0	−2392.9
Random	–	1573.3	−2413.6

[a] '+' represents the detectable probability of the nucleophilic reaction; '–' represents no detectable probability of the nucleophilic reaction.
[b] $E_{binding} = E_{complex} - E_{BSA} - E_{SH}$. E_{BSA} = 3953.9 kcal/mol, E_{SH} = 33.0 kcal/mol.

Molecular recognitions between SH and secondary structures of BSA are also very important. The structures of the complexes reveal some structural features for the binding abilities (Fig. 2 and Table 4). In the complex of SH···BSAβ, remarkably, the distance is 3.37 Å between the oxygen atom (O_{12}) of the hydroxyl group of SH and the carbon atom (C_{34}) of the amide bond of H108 (Leu). Similarly, it can also be found that the distances range from 3.05 to 4.00 Å to most conformations in the complex of SH···BSAβ (Fig. 3). Because the value of van der Waals radii is 3.25 Å between carbon and oxygen atoms, 3.37 Å is within the contact scope for nucleophilic attack on the carbon atom by the oxygen atom which are similar to the situ-

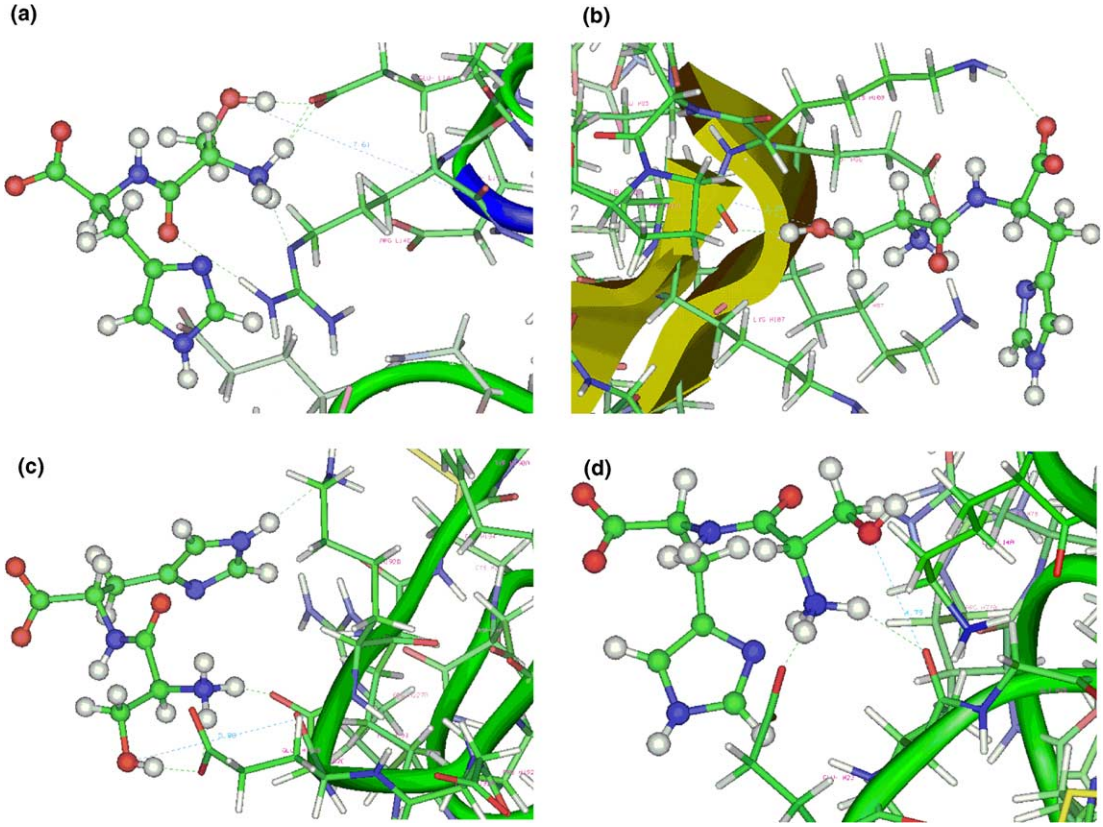

Figure 2. The docked structures of SH with secondary structures of BSA located by performing GRID DOCKING: (a) SH···BSAα, (b) SH···BSAβ, (c) SH···BSA*t*, and (d) SH···BSA*c*. Distances between O and C atoms are marked by cyan lines, H-bonds are marked by green lines.

Table 4. The major structural features in docked complexes between SH and BSA

Entry	Nucleophilic ability of SH	Dist. (Å)[a]	Binding points
Helix	–	7.61	α-NH_3–N=$C(NH_2)_2$ in Arg(L14D) α-NH_3–OCO in Glu^- (L14H) (2H-bonds) HNCO–$(H_2N)_2C$=N in Arg(L14D) OH–OCO in Glu^- (L14H)
Beta	+	3.37	OH–OCNH in Leu(H108) α-NH_3–OCO in Glu^- (H86)(2H-bonds) OCO–H_2N in Lys(H109)
Turn	–	5.80	α-NH_3–OCO in Glu^- (H192B) α-NH_3–OCNH in Gly(H192C) OH–OCO in Glu^- (H192B) Imidazol–H_2N in Lys(H192D)
Random	–	4.79	α-NH_3–OCO in Glu^- (H23) α-NH_3–OCNH in Ile(H24)

[a] Distance between the oxygen atom of the hydroxyl group of SH and the carbon atom of the amide bond.

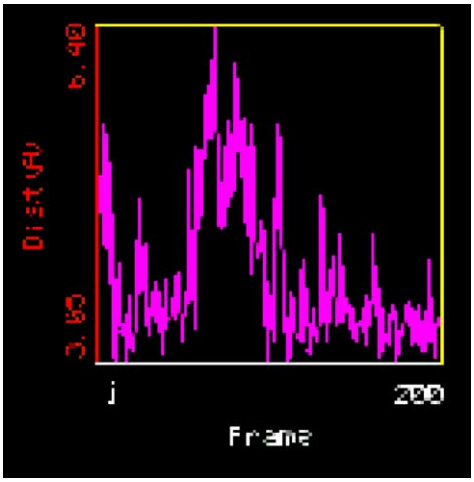

Figure 3. The distance is in the range from 3.05 to 4.00 Å between the oxygen atom of the hydroxyl group of SH and the carbon atom of the amide bond to most conformations extracted from the 200 ps dynamics trajectory in the complex of SH···BSAβ.

ation that SH cleaved DNA.[17] Therefore, it is possible that SH can interact with β-sheets specifically.

In cases of the complexes of SH with α-helix, turn, and random coil, the distances are 7.61, 5.80, and 4.79 Å, respectively. They are beyond the contact range for a nucleophilic attack on carbon by oxygen. So, SH cannot interact with these secondary structures.

In addition, seen from the binding points, in the complex of SH···BSAβ, the hydroxyl group forms one H-bond with the oxygen atom of the amide bond of H108 (Leu). The α-ammonium group of seryl forms two H-bonds with oxygen atoms of the side chain of H86 (Glu). The carboxylic anion of SH forms one H-bond with an amino hydrogen atom of the side chain of H109 (Lys). These interactions may play an active role in keeping the binding geometry and facilitate the nucleophilic attack on carbon by oxygen via bringing SH closer to the β-sheet. However, in the complexes of SH···BSA*t* and SH···BSA*c*, it is the α-ammonium group not the hydroxyl one of seryl that forms one H-bond with the oxygen atom of the amide bond, respectively, so the nucleophilic attack on carbon by oxygen cannot happen. And in the complexes of SH···BSAα and SH···BSA*t*, the interactions between SH and the side chains destroyed the original stable conformations and made the α-helix and turn change into loose coils with low $E_{binding}$ values.

2.3. The results of quantum chemical calculations

For the key part of SH···BSAβ, the results of quantum chemical calculations show that compared to the atomic charges of SH and BSAβ, the negative and positive charges of the oxygen atom (O_{12}) and hydrogen atom (H_{13}) to SH part increased 0.033 and 0.027, respectively (Fig. 4 and Table 5). To BSAβ part, the positive and negative charges of the carbon atom (C_{34}) and oxygen atom (O_{35}) of the carbonyl increased 0.021 and 0.044, respectively. And the negative charges of the nitrogen atom (N_{36}) of the amide bond reduced 0.007. The positive charges of the hydrogen atom (H_{44}) increased 0.01, too. These results indicate that when SH binds to BSAβ, the O_{12} polar effect cause the π–π electronic clouds of the double bond between C_{34} and O_{35} shift from C_{34} to O_{35} greatly, and the p–π electronic clouds of the partial double bond between C_{34} and N_{36} drift from N_{36} to C_{34} obviously. And the deviation extent of σ–*p* electronic clouds between H_{44} and N_{36} is also very strong. That is, these bonds mentioned above are all strongly polarized.

In addition, seen from the natural atomic hybrid percentages in footnotes of Table 5, the C_{34}=O_{35} π-bond and O_{12}–H_{13} σ-bond are also polarized more strongly toward the O_{35} and O_{12}, which have two noteworthy hybrid percentages of 76.15% and 78.00% compared to the situation in SH and BSAβ. The square sums of HOMO coefficients of C_{34} decreased from 8.1×10^{-2} to 1.3×10^{-7}, and the ones of O_{12} did not change. These results indicate that C_{34} can only receive electrons from

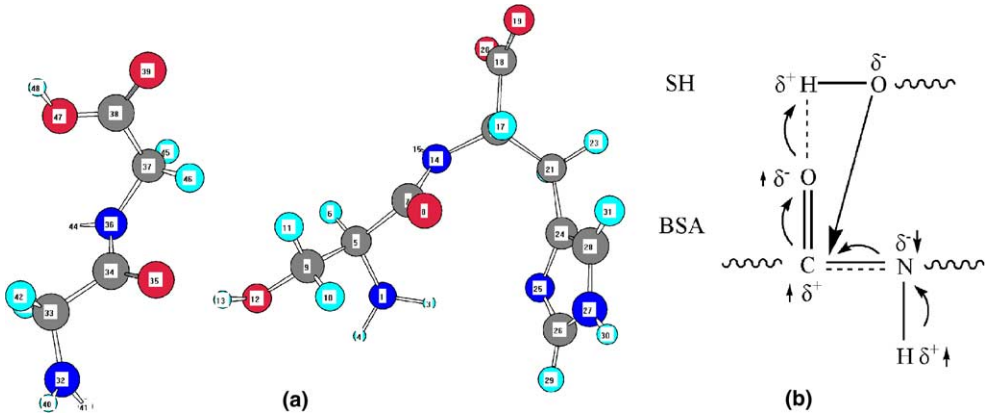

Figure 4. (a) The key part of SH···BSAβ; (b) a scheme about the interaction mode between SH and β-sheets.

Table 5. Natural atomic hybrid percentages,[a] charge distributions and square sums of HOMO coefficients of an amide bond of H108 (Leu) and the hydroxyl of SH calculated by NBO[29] and the population analysis at HF[30]/6-31G*[31]

Entry	SH···BSAβ		SH		BSAβ		ΔQ[b]
	Q[b]	P[c]	Q	P	Q	P	
C_{34}	0.845	1.3×10^{-7}	—[d]	—	0.824	8.1×10^{-2}	0.021
O_{35}	−0.772	—	—	—	−0.728	—	−0.044
N_{36}	−0.756	—	—	—	−0.763	—	0.007
H_{44}	0.431	—	—	—	0.421	—	0.010
O_{12}	−0.860	2.5×10^{-5}	−0.827	2.7×10^{-5}	—	—	−0.033
H_{13}	0.541	—	0.514	—	—	—	0.027

[a] $\%C_{34}$, $\%O_{35}$ and $\%O_{12}$ mean natural atomic hybrid percentages of C_{34}, O_{35} and O_{12}. $\%C_{34}$, $\%O_{35}$ and $\%O_{12}$ of SH···BSAβ are 23.85, 76.15 and 78.00; $\%O_{12}$ of SH is 75.74, $\%C_{34}$ of BSAβ is 28.24.
[b] Q means atomic natural charges. $\Delta Q = Q_{SH\cdots BSA\beta} - Q_{SH\text{ or }BSA\beta}$.
[c] P means square sums of HOMO coefficients.
[d] '—' means no data.

O_{12}. Therefore, it can be deduced that in water solution, the nucleophilic attack on C_{34} by O_{12} is likely and can cause the cleavage of C_{34}–N_{36} bond. And the cleavage mechanism of the peptide bond is similar to that of chymotrypsin.[5,27,28]

2.4. The relative relations between the nucleophilic ability of SH and the ratio of the content of β-sheets to that of α-helices

We also used the crystal structures of lysozyme and PrP^c to dock with SH, respectively. In Table 6, the higher binding energies between SH and β-sheets showed that

Table 6. The binding energies of SH with secondary structures of lysozyme or PrP^c (kcal/mol)

Entry	Nucleophilic ability of SH[a]	Lysozyme (132L)		PrP^c (1DWY)	
		$E_{complex}$	$E_{binding}$[b]	$E_{complex}$	$E_{binding}$
Helix	—	−322.4	−216.7	−39.7	−669.4
Beta	—	−299.7	−194.0	−1.2	−630.9
Turn	—	−316.5	−210.8	−76.0	−705.7
Random	—	−270.9	−165.2	32.7	−597.0

[a] '—' represents no detectable probability of the nucleophilic reaction.
[b] $E_{binding} = E_{complex} - E_{lys\text{ or }PrPc} - E_{SH}$.
[c] $E_{lys} = -138.7$ kcal/mol, $E_{PrPc} = 596.7$ kcal/mol, $E_{SH} = 33.0$ kcal/mol.

the nucleophilic reaction of SH was unfavorable when the content of β-sheets was smaller than that of α-helices greatly. And seen from the binding points in Table 7, SH mainly interacted with the side chains of lysozyme and PrP^c. The chemical interaction between the oxygen atom of the hydroxyl group of SH and the carbon atom of the amide bond was impossible. The hydrogen bonds of β-sheets could not be broken.

Therefore, all the results of CD experiments and molecular modeling are summed up in Table 8. From the results, it can be deduced that the ability that SH causes the breakage of hydrogen bonds of β-sheets is related to the ratio of the content of β-sheets to that of α-helices in a protein. When the ratio is greater than 0.6, SH can break the hydrogen bonds of β-sheets whether in solution or in crystal states. While the ratio is smaller than 0.2, SH cannot break the hydrogen bonds of β-sheets. For example, SH cannot interact with PrP^c because it is a highly helical (49.1%) with virtually no β-sheet structure (3.6%). In contrast, PrP^{Sc} contains a large amount of β-sheet structure (43%) and less helical structure (30%). If SH interact with PrP^{Sc}, the hydrogen bonds of β-sheets can be broken and result in the conversion of β-sheets to other secondary structures. So, SH can be a hopeful therapeutic agent to prion diseases.

Table 7. The major binding points in docked complexes between SH and lysozyme (132L) or PrP[c] (1DWY)

Entry	Lysozyme (132L)	PrP[c] (1DWY)
Helix	α-NH_3–OCNH in Ala (10) α-NH_3–N=$C(NH_2)_2$ in Arg (14) OCO–HOCO in Asp (87) (2H-bonds) OCO–Imidazol in His (15)	α-NH_3–OCO in Glu^- (A211) OCO–H_2N in Gln (A172) OCO–H_2N in Gln (A219) (2H-bonds) OH–OH in Thr (A216) Imidazol–H_2N in Asn (A173)
Beta	α-NH_3–$OCNH_2$ in Asn (44) OCO–HO in Thr (43) OCO–HNCO in Arg (45) OCO–$(H_2N)_2C$=N in Arg (68) (2H-bonds) OCNH–OCNH in Thr (43)	α-NH_3–OCNH in Gly (A131) α-NH_3–$OCNH_2$ in Gln (A160) HNCO–H_2NCO in Gln (A160)
Turn	α-NH_3–$OCNH_2$ in Asn (113) α-NH_3–OCNH in Lys (116) OCO–$(H_2N)_2C$=N in Arg (21) (2H-bonds) OCO–HOC_6H_4 in Tyr (23) OCO–H_2NCO in Asn (106) OH–N=$C(NH_2)_2$ in Arg (112) Imidazol–H_2N in Lys (116)	α-NH_3–OCO in Glu^- (A152) α-NH_3–$OCNH_2$ in Asn (A153) OH–OCO in Glu^- (A152) Imidazol–N=$C(NH_2)_2$ in Arg (A148)
Random	α-NH_3–HOC_6H_4 in Tyr (53) α-NH_3–OCNH in Asp (66) α-NH_3–N=$C(NH_2)_2$ in Arg (68) OCO–HNCO in Arg (68) OCO–$(H_2N)_2C$=N in Arg (68) CONH–$(NH_2)_2C$=N in Arg (68)	α-NH_3–OCNH in Leu (A125) α-NH_3–OCNH in Gly (A126)

Table 8. The relative relations between the nucleophilic ability of SH and the ratio of %Beta[a] to %Helix[a]

Entry	In solution state				In crystal state	
	%Beta	%Helix	R[b]	Ability[c]	R	Ability
BSA	26.5	45.7	0.6	+ +[d]	2.9	+ + +
Lysozyme	53.2	14.1	3.8	+ + + +	0.2	–[d]
PrP[c]	—[e]	—	—	—	0.1	–

[a] %Beta and %Helix represent the content of β-sheets and that of α-helices, respectively. They are 29.7, 10.4 in BSA (1C1U); 6.2, 31.0 in lysozyme (132L); 3.6, 49.1 in PrP[c] (1DWY), respectively.
[b] R means the ratio of %Beta to %Helix.
[c] Ability means the nucleophilic one of SH.
[d] A '+' represents approximately 5% β-sheets can be decreased; '–' represents no change of %Beta.
[e] '—' means no data.

3. Conclusion

In this paper, CD spectra indicate that SH can break the hydrogen bonds of β-sheets selectively and result in the conversion of β-sheets to other secondary structures. The results of molecular modeling and quantum chemical calculations demonstrate the key structural features and the bonding situation for the interaction mode between SH and β-sheets. A minimum binding energy, a contact O–C distance, and multiple binding sites are all necessary for the nucleophilic ability of SH. Natural charges, natural atomic hybrid percentages and square sums of HOMO coefficients of an amide bond of H108 (Leu) and the hydroxyl of SH calculated by the NBO and population analysis at HF/6-31G* support the suggested interaction mode between SH and β-sheets. Together with the result of PAGE, we conclude that it is possible that SH can cleave a protein specifically at β-sheet. In the future work, we will modify the structure of SH and realize the specific cleavage to proteins.

4. Experimental

4.1. Material and methods

BSA (MW = 66 kDa, 583 amino acids[32]), lysozyme (MW = 14.3 kDa, 129 amino acids) and SH were purchased from Beijing Xiasi Biotechnology Limited Company of China and American ICN Biological Reagent Company, respectively.

The solutions of BSA, lysozyme, SH, and NaCl were prepared by dissolving the appropriate amount of the samples in deionized water, and pH ranged from 6.0 to 7.0. No buffer was used.[15] The concentrations of the concentrated solutions were 2.0 mg/mL, 14.3 mg/mL, 7.02 mM, and 6.50 mM, respectively. NaCl solution was used to keep the ionic strength[21] and stabilize the CD spectra.

The CD control experiment of BSA was carried out using 1 mL BSA solution containing 10 μL BSA, 500 μL NaCl and 490 μL H_2O. The dilute concentration (C_{exptl}) of BSA was 0.02 mg/mL.

And the CD control experiment of lysozyme was carried out using 1 mL lysozyme solution containing 50 μL

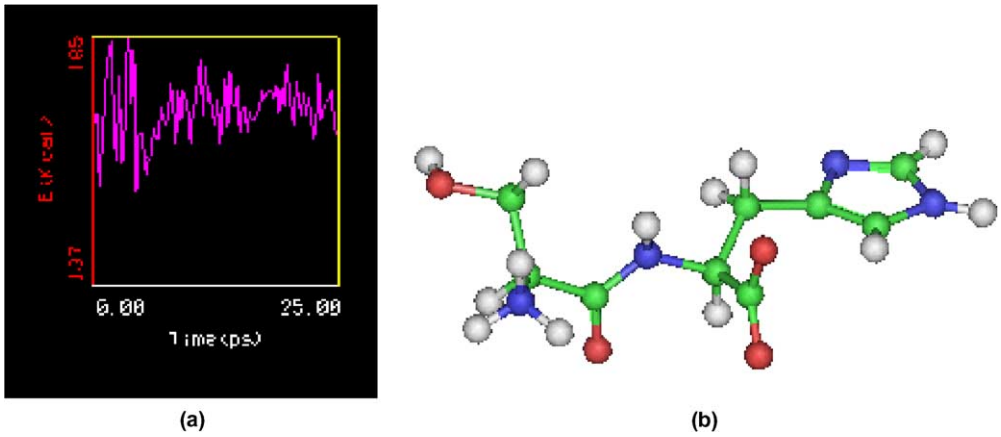

Figure 5. (a) MD energetic equilibrium pictures of SH; (b) the most stable conformation of SH with $E = 33.0$ kcal/mol.

lysozyme, 500 μL NaCl and 450 μL H_2O. The dilute concentration (C_{exptl}) of lysozyme was 0.72 mg/mL.

The titration of SH to proteins was used. After 10 μL SH solution was titrated into 1 mL protein solution, the water volume used was reduced 10 μL to keep the 1 mL constant total volume. The incubation time was about 5 min at 298 K until the solution reached the equilibrium state. Then the CD spectra were recorded.

The CD spectra were recorded on a J-715 spectropolarimeter, with a bandwidth 2.0 nm, and the response time was 1 s. A quartz microcell with a 1-mm path length was used to load the sample. Each spectrum was obtained by accumulating one to two scans. The same experiments were repeated five times. The spectra were analyzed using J-700 system software supplied by Jasco.[33] At first, the mean residue concentrations (C_{mean}) of BSA and lysozyme were calculated with Eq. 1 and the unit is mol/L. The Standard Analysis module implemented in the software of Jasco[33] was used to calculate molar ellipses of CD spectra. At last, the Secondary Structure Estimation module[33] implemented in the same software of Jasco was used to calculate the percentages of secondary structures of BSA and lysozyme.

$$C_{mean} = C_{exptl} \cdot \text{number of amino acids/MW} \qquad (1)$$

4.2. Molecular modeling

All molecular modeling studies were performed on a Silicon Graphics O2 computer running MSI InsightII software.[34,35] The CVFF[36] force field was used.

Energy minimizations for the crystal structure of BSA (1C1U), lysozyme (132L) and PrP^c (1DWY) were performed using the standard steepest descent and conjugated gradients minimization algorithms. A 1.5 nm cut-off distance was applied to calculate the non-bond interaction with spline width 1.0 Å and buffer width 0.5 Å, respectively.

SH was built manually using the InsightII builder module and the amide bond was set to be *trans*. SH was first minimized. Then the system was heated to 800 K for 5 ps, and the molecular dynamics (MD) trajectories for 20 ps were kept using Discover module. The time was proved to be enough long because the total energies of most conformations had reached equilibrium states (Fig. 5a). A time step of 1 fs was used and the coordinates were written to the history file every 250 steps. Then the procedures of cluster analysis and minimization were applied to the resulting conformers. The most stable conformation of SH is shown in Figure 5b. Its bond lengths and bond angles are in agreement with general dipeptides.

For minimized BSA (1C1U), cylinder 1 of α helices from L14D (Arg) to L14J (Tyr), a part of ribbon 8 from H85 (Leu) to H90 (Ile) and ribbon 9 from H104 (Ala) to H108 (Leu) of β-sheets, ribbon 15 of turns from H192 (Pro) to H192C (Gly), ribbon 6 of random coils from H18 (Glu^-) to H28 (Pro) were selected to dock with SH, respectively. The initial three-dimensional structures of the complexes between SH and the secondary structures of BSA (1C1U) were generated manually by placing SH near alpha helices, β-sheets, turns, or random coils on the exterior surface of BSA (1C1U), respectively.[37] The positions of SH were scanned by moving it manually on the screen. In order to guarantee SH to move freely, it could not be placed into the interior of BSA (1C1U). Then defining subsets for the binding sites and creating assemblies of ligands and receptors. At last, using Affinity program[38] of Docking module to perform the grid docking command. After the grid was set up, the complex was minimized. The amide bond of SH was defined a torsion to prevent it from inverting to *cis* conformations. To each complex, five binding structures were searched which were within 10 kcal/mol of the lowest energy structure having been found.

Select a structure early and frequently found with a *trans* amide bond of SH as the starting docking conformation for further MD simulation. After the initial 5 ps heating period and the temperature stabilization, MD trajectories were run for 200 ps when were proved to be enough long because the total energies of most conformations

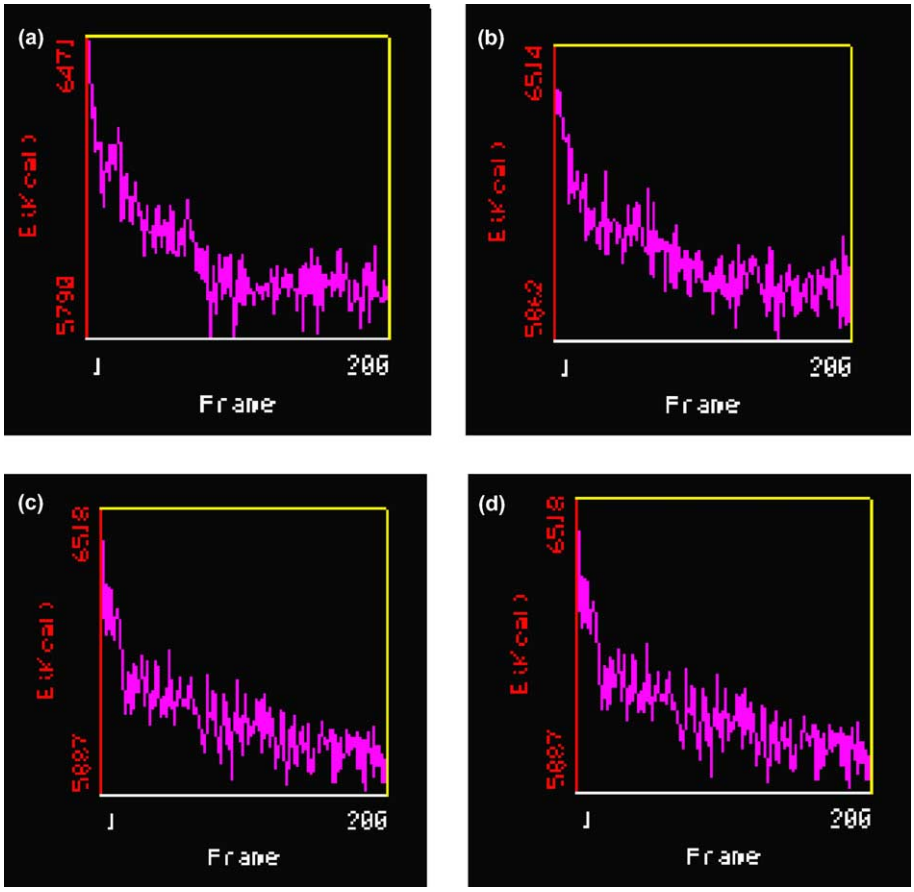

Figure 6. MD energetic equilibrium pictures: (a) SH···BSAα, (b) SH···BSAβ, (c) SH···BSA*t*, and (d) SH···BSA*c*.

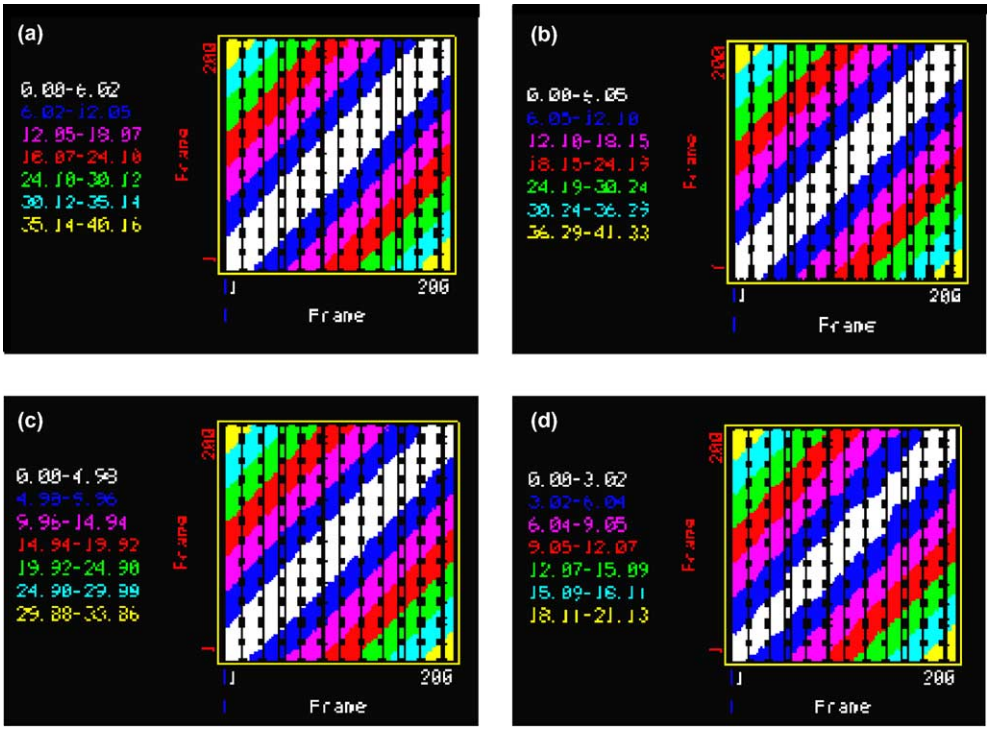

Figure 7. MD three-dimensional graphs of cluster analyses: (a) SH···BSAα, (b) SH···BSAβ, (c) SH···BSA*t*, and (d) SH···BSA*c*. Each color represents a group of similar conformations. The lower the RMS, the more similar the conformation.

had reached equilibrium states (Fig. 6). A time step of 1 fs was used and the coordinates were saved at every 1 ps. During the MD simulations, the amide bond of SH was kept *trans*.

For each complex, the 200 structures were clustered into seven conformational families according to the backbone structural similarities. Each point represents the RMS comparison of two conformations (Fig. 7). The points in white regions with a low RMS (0.00–2.00) around the diagonals represent the largest amount of similar conformations. Select some white data points and minimize the energies of the corresponding conformers. The four conformers with the lowest total energies were found for SH···BSAα, SH···BSAβ, SH···BSA*t* and SH···BSA*c* (Fig. 2).

To the complexes between SH and lysozyme (132L) or PrP^c (1DWY), the similar calculations were performed. The results were included in Tables 6 and 7.

4.3. Quantum chemical calculations

In order to investigate the cleaved mechanism of the amide bond of BSA (1C1U), the key part of H108 (Leu), H109 (Lys), and SH of SH···BSAβ was chosen as the object of the quantum chemical calculations implemented in Gaussian 98[39] suite of programs. The side chains of the two amino acids were substituted with hydrogen atoms to guarantee a kind of sufficiently accurate calculation of the wavefunction.[30] A hydrogen atom and a hydroxyl group whose bond lengths, bond angles and dihedral angles were obtained from the structure of SH···BSAβ were added to the N-terminal and C-terminal to keep its electronic neutrality. HF/6-31G* were used to calculate natural charges. The natural population analysis was used to analyze the bonding situation.

Acknowledgements

Thank for the financial supports from Chinese National Science Foundation (No. 20132020), the Ministry of Science and Technology, the Chinese Ministry of Education and Tsinghua University.

Supplementary data

The coordinates of structures shown in Figures 2(a), 2(b), 2(c), 2(d) and 5b in pdb formats are available. Supplementary material associated with this article can be found, in the online version, at doi:10.1016/j.bmc.2004.12.047.

References and notes

1. Radzicka, A.; Wolfende, R. *J. Am. Chem. Soc.* **1996**, *118*, 6105.
2. Barrett, A. J. *Handbook of Proteolytic Enzymes*; Academic: London, 1998.
3. Fersht, A. *Enzyme Structure and Mechanism*, 2nd ed.; Freeman: New York, 1985; p 405.
4. Sternlicht, M. D.; Werb, Z. *Annu. Rev. Cell. Dev. Biol.* **2001**, *17*, 463.
5. Hedstrom, L. *Chem. Rev.* **2002**, *102*, 4501.
6. Dodson, G.; Wlodawr, A. *Trends Biochem. Sci.* **1998**, *23*, 347.
7. Li, Y.; Zhao, Y.-F.; Hatfield, S.; Wan, R.; Zhu, Q.; Li, X.; McMills, M.; Ma, Y.; Li, J.; Brown, K. L.; He, C.; Liu, F.; Chen, X. *Bioorg. Med. Chem.* **2000**, *8*, 2675.
8. Croft, L. R. In *Handbook of Protein Sequence Analysis*, 2nd ed.; Wiley: Chichester, 1980.
9. Kumar, C. V.; Buranaprapuk, A. *J. Am. Chem. Soc.* **1999**, *121*, 4262.
10. Ding, F.; Borreguero, J. M.; Buldyrey, S. V.; Stanley, H. E.; Dokholyan, N. V. *Proteins Struct. Funct. Genet.* **2003**, *53*, 220.
11. Safar, J. *Seminars in Virology* **1996**, *7*, 207.
12. Stoppini, M.; Andreola, A.; Foresti, G.; Bellotti, V. *Pharm. Res.* **2004**, *50*, 419.
13. Skribanek, Z.; Baláspiri, L.; Mák, M. *J. Mass. Spectrom.* **2001**, *36*, 1226.
14. Qiao, F.; Hu, J.; Zhu, H.; Luo, X.; Zhu, L.; Zhu, D. *Polyhedron* **1999**, *18*, 1629.
15. Chen, J.; Wan, R.; Liu, H.; Jiang, Y.; Zhao, Y.-F. *Chem. J. Chin. Univ.* **2001**, *21*, 1349.
16. Du, H.-L.; Wang, Y.-T.; Yang, L.-F.; Luo, W.-X.; Xia, N.-S.; Zhao, Y.-F. *Lett. Pept. Sci.* **2002**, *9*, 5.
17. Sun, M.; Ma, Y.; Ji, S.; Liu, H.; Zhao, Y.-F. *Bioorg. Med. Chem. Lett.* **2004**, *14*, 3711.
18. Gelamo, E. L.; Silva, C. H. T. P.; Imasato, H.; Tabak, M. *Biochim. Biophys. Acta* **2002**, *1594*, 84.
19. Kosa, T.; Maruyama, T.; Otagiri, M. *Pharm. Res.* **1997**, *14*, 1607.
20. Moreno, F.; Cortijo, M.; Jimenez, J. G. *Photochem. Photobiol.* **1999**, *69*, 8.
21. Tian, J.; Liu, J.; Tian, X.; Hu, Z.; Chen, X. *J. Mol. Struct.* **2004**, *691*, 197.
22. Nordtveit, R. J.; Vårum, K. M.; Smidsrød, O. *Carbohydr. Polym.* **1996**, *29*, 163.
23. Balfry, S. K.; Iwama, G. K. *Comp. Biochem. Physiol. B* **2004**, *138*, 207.
24. Walton, A. G. *Polypeptides and Protein Structure*; Elsevier: New York, 1981; pp 17–49.
25. Fasman, G. D. In *The Development of the Prediction of Protein Structure*; Fasman, G. D., Ed.; Plenum: New York, 1989; pp 359–390.
26. Daggett, V. *Curr. Opin. Biotechnol.* **1998**, *9*, 359.
27. Reuter, N.; Monard, G.; Cartier, A.; Maigret, B. *J. Mol. Graph. Model.* **1997**, *15*, 394.
28. Silva, F. P., Jr.; De-Simone, S. G. *Bioorg. Med. Chem.* **2004**, *12*, 2571.
29. Glendening, E. D.; Reed, A. E.; Carpenter, J. E.; Weinhold, F. NBO Version 3.1; Irvine, CA.
30. Höltje, H.-D.; Folkers, G. *Molecular Modeling Basic Principles and Applications*; VCH: Weinheim, 1996; p 39.
31. Hehre, W. J.; Radom, L.; Schleyer, P. v. R.; Pople, J. A. *Ab Initio Molecular Orbital Theory*; Wiley–Interscience: New York, 1986.
32. Li, A.; Sowder, R. C., II; Henderson, L. E.; Moore, S. P.; Garfinkel, D. J.; Fisher, R. J. *Anal. Chem.* **2001**, *73*, 5395.
33. McPhie, P. *Anal. Biochem.* **2001**, *293*, 109.
34. Molecular Simulations Inc., (MSI). InsightII 2000.1, San Diego, CA, 2000.
35. Molecular Simulations Inc., (MSI). Discover_3 version 2.98, San Diego, CA, 1997.
36. Dauber-Osguthorpe, P.; Roberts, V. A.; Osguthorpe, D. J.; Wolff, J.; Genest, M.; Hagler, A. T. *Proteins Struct. Funct. Genet.* **1988**, *4*, 31.

37. Cavillon, F.; Elhaddaoui, A.; Alix, A. J. P.; Turrell, S.; Dauchez, M. *J. Mol. Struct.* **1997**, *408–409*, 185.
38. Molecular Simulations Inc., (MSI). Affinity, San Diego, CA, 1998.
39. Frisch, M. J.; Trucks, G. W.; Schlegel, H. B.; Scuseria, G. E.; Robb, M. A.; Cheeseman, J. R.; Zakrzewski, V. G.; Montgomery, J. A., Jr.; Stratmann, R. E.; Burant, J. C.; Dapprich, S.; Millam, J. M.; Daniels, A. D.; Kudin, K. N.; Strain, M. C.; Farkas, O.; Tomasi, J.; Barone, V.; Cossi, M.; Cammi, R.; Mennucci, B.; Pomelli, C.; Adamo, C.; Clifford, S.; Ochterski, J.; Petersson, G. A.; Ayala, P. Y.; Cui, Q.; Morokuma, K.; Malick, D. K.; Rabuck, A. D.; Raghavachari, K.; Foresman, J. B.; Cioslowski, J.; Ortiz, J. V.; Baboul, A. G.; Stefanov, B. B.; Liu, G.; Liashenko, A.; Piskorz, P.; Komaromi, I.; Gomperts, R.; Martin, R. L.; Fox, D. J.; Keith, T.; AlLaham, M. A.; Peng, C. Y.; Nanayakkara, A.; Gonzalez, C.; Challacombe, M.; Gill, P. M. W.; Johnson, B. G.; Chen, W.; Wong, M. W.; Andres, J. L.; Head-Gordon, M.; Replogle, E. S.; Pople, J. A. Gaussian 98. Revision A.9. Gaussian Inc., Pittsburgh, PA, 1998.